CONTROL OF A DOUBLY-FED INDUCTION GENERATOR FOR WIND ENERGY CONVERSION SYSTEMS.

F. Poitiers, M. Machmoum, R. Le Doeuff and M.E. Zaim

GE44-LARGE, Ecole Polytechnique de l'Université de Nantes, Saint Nazaire, France
Corresponding author : F. Poitiers email : poitiers@esa-igelec.univ-nantes.fr

Abstract

This paper deals with a variable speed device to produce electrical energy on a power network, based on a doubly-fed induction machine used in generating mode (DFIG). This device is intended to equip nacelles of wind turbines. First, a mathematical model of the machine written in an appropriate d-q reference frame is established to investigate simulations. In order to control the power flowing between the stator of the DFIG and the power network, a control law is synthesized using two types of controllers : PI and RST. Their respective performances are compared in terms of power reference tracking, response to sudden speed variations, sensitivity to perturbations and robustness against machine parameters variations.

NOMENCLATURE

$\mathbf{V_{ds}}$, $\mathbf{V_{qs}}$, $\mathbf{V_{dr}}$, $\mathbf{V_{qr}}$: Two-phase statoric and rotoric voltages.
$\mathbf{\Psi_{ds}}$, $\mathbf{\Psi_{qs}}$, $\mathbf{\Psi_{dr}}$, $\mathbf{\Psi_{qr}}$: Two-phase statoric and rotoric fluxes.
$\mathbf{I_{ds}}$, $\mathbf{I_{qs}}$, $\mathbf{I_{dr}}$, $\mathbf{I_{qr}}$: Two-phase statoric and rotoric currents.
θ_s , θ_r : Statoric flux position and mechanical rotoric position.
$\mathbf{\Omega}$: Mechanical speed.
$\mathbf{\Gamma_m}$, $\mathbf{\Gamma_e}$: Prime mover and electromagnetic torque.
P : Number of pole pairs.
$\mathbf{R_s}$, $\mathbf{R_r}$: Per phase statoric and rotoric resistances.
M : Magnetizing inductance.
$\mathbf{L_s}$, $\mathbf{L_r}$: Total cyclic statoric and rotoric inductances.
g : generator slip.
J, f : Inertia and viscous friction.
p : Laplace operator.

1. INTRODUCTION

In order to meet power needs, taking into account economical and environmental factors, wind energy conversion is gradually gaining interest as a suitable source of renewable energy. The electromagnetic conversion is usually achieved by induction machines or synchronous and permanent magnet generators. Squirrel cage induction generators are widely used because of their lower cost, reliability, construction and simplicity of maintenance [1]. But when it is directly connected to a power network, which imposes the frequency, the speed must be set to a constant value by a mechanical device on the wind turbine. Then, for a high value of wind speed, the totality of the theoretical power can not be extracted. To overcome this problem, a converter, which must be dimensioned for the totality of the power exchanged, can be placed between the stator and the network. In order to enable variable speed operations with a lower rated power converter, doubly-fed induction generator (DFIG) can be used as shown on Fig. 1. The stator is directly connected to the grid and the rotor is fed to magnetize the machine.

In this paper, the control of electrical power exchanged between the stator of the DFIG and the power network by controlling independently the torque (consequently the active power) and the reactive power is presented [2]. Several investigations have been developed in this direction using cycloconverters as converters and classical proportional-integral regulators [3-5]. In our case, after modeling the DFIG and choosing the appropriate d-q reference frame, active and reactive powers are controlled using respectively Integral-Proportional (PI) and an RST controller based on pole placement theory. Their performances are compared in terms of reference tracking, sensitivity to perturbations and robustness against machine's parameters variations.

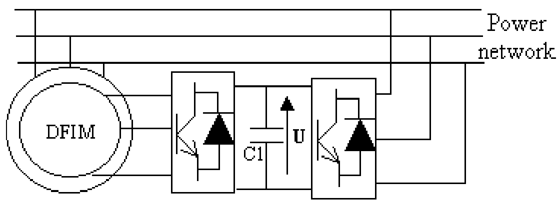

Fig. 1 Doubly-fed induction generator

2. MATHEMATICAL MODEL OF THE DFIG

For a doubly fed induction machine, the Concordia and Park transformation's application to the traditional a,b,c model allows to write a dynamic model in a d-q reference frame as follows:

$$\begin{cases} V_{ds} = R_s I_{ds} + \frac{d}{dt}\psi_{ds} - \dot{\theta}_s \psi_{qs} \\ V_{qs} = R_s I_{qs} + \frac{d}{dt}\psi_{qs} + \dot{\theta}_s \psi_{ds} \\ V_{dr} = R_r I_{dr} + \frac{d}{dt}\psi_{dr} - \dot{\theta}_r \psi_{qr} \\ V_{qr} = R_s I_{qr} + \frac{d}{dt}\psi_{qr} + \dot{\theta}_r \psi_{dr} \end{cases} \tag{2.1}$$

$$\begin{cases} \psi_{ds} = L_s I_{ds} + M I_{dr} \\ \psi_{qs} = L_s I_{qs} + M I_{qr} \\ \psi_{dr} = L_r I_{dr} + M I_{ds} \\ \psi_{qr} = L_r I_{qr} + M I_{qs} \end{cases} \tag{2.2}$$

$$\Gamma_m = \Gamma_e + J \frac{d\Omega}{dt} + f\Omega \tag{2.3}$$

$$\Gamma_e = -P \frac{M}{L_s} (\psi_{qs} I_{dr} - \psi_{ds} I_{qr}) \tag{2.4}$$

3. DFIG CONTROL

3.1 Aim of the control

When the DFIG is connected to an existing network, this connection must be done in three steps which are presented below [6]. The first step is the regulation of the statoric voltages with the network voltages as reference (figure 2). The second step is the stator connection to this network. As the voltages of the two devices are synchronized, this connection can be done without problem. Once this connection is achieved, the third step, which constitutes the topic of this paper, is the power regulation between the stator and the network. (figure 3).

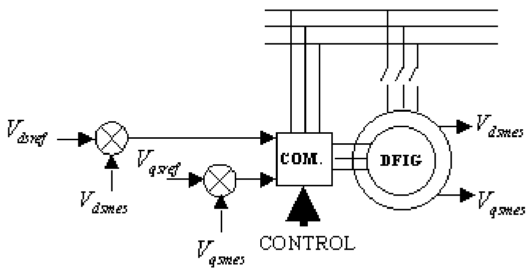

Fig. 2 : First step of the DFIG connection

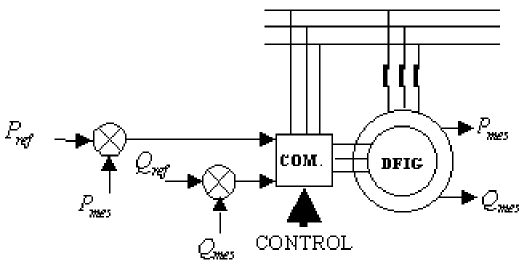

Fig. 3 : Third step of the DFIG connection

For a given wind turbine, some relations exist between the wind speed, the generator's rotating speed and the available mechanical power (figure 4). If the wind speed is measured and the mechanical characteristics of the wind turbine are known, it is possible to deduce in real-time the theoretical electrical power which can be generated. It is then possible to control the generator using this power as reference.

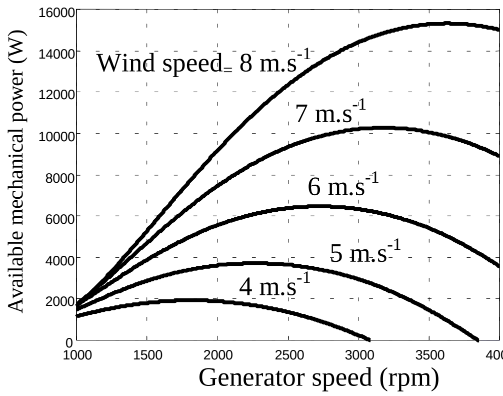

Fig. 4 : Example of wind-turbine power-curves

3.2 Establishment of the control strategy

To achieve a stator active and reactive power vector control as shown on figure 3, we choose a d-q reference-frame synchronized with the stator flux (figure 5) [7]. By setting the statoric flux vector aligned with d-axis, we have :

$$\psi_{ds} = \psi_s \text{ and } \psi_{qs} = 0 \tag{3.1}$$

$$\Gamma_e = -p \frac{M}{L_s} I_{qr} \psi_{ds} \tag{3.2}$$

The electromagnetic torque and then the active power will only depend on the q-axis rotoric current. Neglecting the per phase statoric resistance R_s (that's the case for medium power machines used in wind energy conversion systems), the statoric voltage of the phase number n of the DFIG can be written as follows:

$$V_{sn} \simeq \frac{d\psi_{sn}}{dt} \;\; ; \;\; \text{n=a, b or c.} \tag{3.3}$$

The statoric voltage vector is consequently in quadrature advance in comparison with the statoric flux vector. Then we can write :

$$V_{ds} = 0 \text{ and } V_{qs} = V_s \tag{3.4}$$

In order to elaborate transformation angles for statoric and rotoric variables, the statoric pulsation and the mechanical speed must be measured (figure 6). The setting of different vectors and transformation angles deduced from these measurements is represented on figure 5. θ_1 and θ_2 are used in Park matrix to convert statoric and rotoric two-phase rotating variables into two-phase fixed variables and reciprocally.

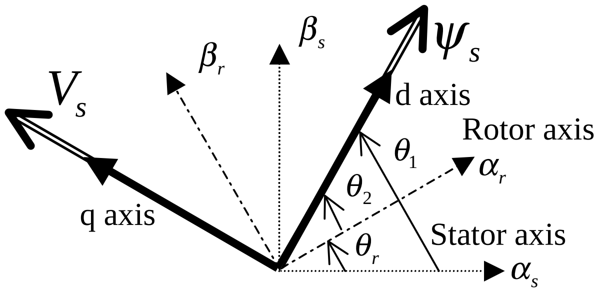

Fig. 5 : Setting of vectors and transformation angles

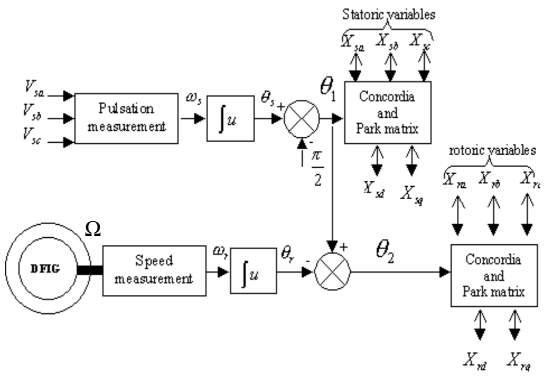

Fig. 6 : Determination of transformation angles

By choosing this reference frame, statoric voltages and fluxes can be rewriten as follows :

$$\begin{cases} V_{ds} = 0 & ; \quad V_{qs} = V_s = \omega_s \psi_{ds} \\ \psi_{ds} = 0 = L_s I_{qs} + M I_{qr} & ; \quad \psi_{dr} = L_r I_{dr} + M I_{ds} \\ \psi_{qs} = \psi_s = L_s I_{ds} + M I_{dr} & ; \quad \psi_{qr} = L_r I_{qr} + M I_{qs} \end{cases} \tag{3.5}$$

The statoric active and reactive power, the rotoric fluxes and voltages can be written versus rotoric currents as:

$$\begin{cases} P = -V_s \dfrac{M}{L_s} I_{qr} \\ Q = \dfrac{V_s \psi_s}{L_s} - \dfrac{V_s M}{L_s} I_{dr} \end{cases} \tag{3.6}$$

$$\begin{cases} \psi_{dr} = (L_r - \dfrac{M^2}{L_s}) I_{dr} + \dfrac{M V_s}{\omega_s L_s} \\ \psi_{qr} = (L_r - \dfrac{M^2}{L_s}) I_{qr} \end{cases} \tag{3.7}$$

$$\begin{cases} V_{dr} = R_r I_{dr} + (L_r - \dfrac{M^2}{L_s}) \dfrac{dI_{dr}}{dt} - g\omega_s (L_r - \dfrac{M^2}{L_s}) I_{qr} \\ V_{qr} = R_r I_{qr} + (L_r - \dfrac{M^2}{L_s}) \dfrac{dI_{qr}}{dt} + g\omega_s (L_r - \dfrac{M^2}{L_s}) I_{dr} + g\omega_s \dfrac{MV_s}{\omega_s L_s} \end{cases} \tag{3.8}$$

In steady state, the second derivative terms of the two equations in (3.8) are nil. The third terms, which constitutes cross-coupling terms can be neglected because of their small influence. Knowing relations (3.6) and (3.8), it is possible to synthesize the regulators and establish the global block-diagram of the controlled system (figure 7).

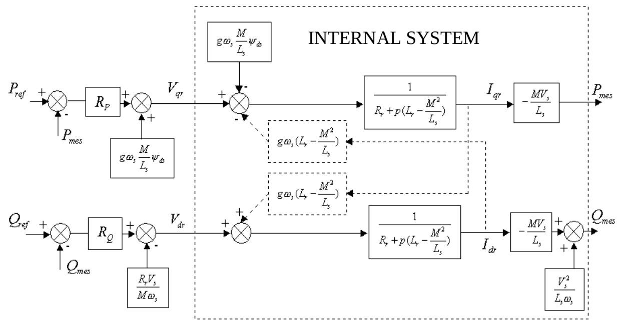

Fig. 7 : Power control of DFIG

The blocks R_P and R_Q represent active and reactive power regulators. The aim of these regulators is to obtain high dynamic performances in terms of reference tracking, sensitivity to perturbations and robustness. To realize these objectives, two types of regulators are studied and compared : Proportional Integral and RST controller based on pole placement theory [8]. Assuming that the cross-coupling terms (represented on dashed lines) are neglected, rotoric currents are then directly related to active and reactive power by constant terms. Then, internal current-control loops are not necessary. The synthesis of Proportional-integral controller is achieved by the classical method of pole compensation and will not be detailed afterwards. The RST controller synthesis is detailed below.

3.3 RST controller synthesis

The block-diagram of a system with its RST controller is presented on figure 8.

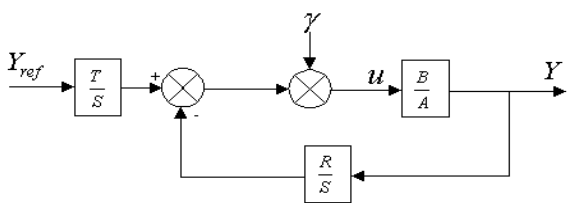

Fig. 8 : Block diagram of the RST controller.

The system with the transfer-function $\frac{B}{A}$ has Y_{ref} as reference and is disturbed by the variable γ. R, S and T are polynomials which constitutes the controller. In our case, we have :

$$A = L_s R_r + pL_s(L_r - \frac{M^2}{L_s}) \text{ and } B = MV_s \quad (3.9)$$

Where p is the Laplace operator.
The transfer-function of the regulated system is :

$$Y = \frac{BT}{AS+BR} Y_{ref} + \frac{BS}{AS+BR}\gamma \quad (3.10)$$

By applying the Besout equation, we put :

$$D = AS + BR = CF \quad (3.11)$$

Where C is the command polynomial and F is the filtering polynomial. In order to have a good adjustment accuracy, we choose a strictly proper regulator. So if A is a polynomial of n degree (deg(A)=n) we must have :

deg(D)=2n+1
deg(S)=deg(A)+1
deg(R)=deg(A).

In our case :

$$\begin{cases} A = a_1 p + a_0 & ;\ R = r_1 p + r_0 \\ B = b_0 & ;\ S = s_2 p^2 + s_1 p + s_0 \\ D = d_3 p^3 + d_2 p^2 + d_1 p + a_0 \end{cases} \quad (3.12)$$

To find the coefficients of polynomials R and S, the robust pole placement method is adopted with T_c as control horizon and T_f as filtering horizon [8]. We have :

$$p_c = -\frac{1}{T_c} \text{ and } p_f = -\frac{1}{T_f} \quad (3.13)$$

where p_c is the pole of C and p_f the double pole of F. The pole p_c must accelerate the system and is generally chosen three to five times greater than the pole of A p_a. p_f is generally chosen three times smaller than p_c. In our case :

$$T_c = \frac{1}{3} T_f = -\frac{1}{3p_a} = \frac{L_s(L_r - \frac{M^2}{L_s})}{5L_s R_r} \quad (3.14)$$

Perturbations are generally considered as piecewise constant. γ can then be modeled by a step input. To obtain good disturbance rejections, the final value theorem indicate that the term $\frac{BS}{AS+BR}$ must tend towards zero:

$$\lim_{p \to 0} p \frac{S}{D}\frac{\gamma}{p} = 0 \quad (3.15)$$

To obtain a good stability in steady-state, we must have $D(0) \neq 0$ and respect relation (3.15). The Bezout equation leads to four equations with four unknown terms where the coefficients of D are related to the coefficients of polynomials R and S by the Sylvester Matrix :

$$\begin{pmatrix} d_3 \\ d_2 \\ d_1 \\ d_0 \end{pmatrix} = \begin{pmatrix} a_1 & 0 & 0 & 0 \\ 0 & a_1 & 0 & 0 \\ 0 & a_0 & b_0 & 0 \\ 0 & 0 & 0 & b_0 \end{pmatrix} \begin{pmatrix} s_2 \\ s_1 \\ r_1 \\ r_0 \end{pmatrix} \quad (3.16)$$

In order to determine the coefficients of T, we consider that in steady state Y must be equal to Y_{ref} so:

$$\lim_{p \to 0} \frac{BT}{AS+BR} = 1 \quad (3.17)$$

As we know that S(0)=0, we conclude that T=R(0). In order to separate regulation and reference tracking, we try to make the term $\frac{BT}{AS+BR}$ only dependent on C. We then consider T=hF (where h is real) and we can write :

$$\frac{BT}{AS+BR} = \frac{BT}{D} = \frac{BhF}{CF} = \frac{Bh}{C} \quad (3.18)$$

As T=R(0), we conclude that $h = \frac{R(0)}{F(0)}$.

4. REGULATORS PERFORMANCES

In this part, simulations are investigated with a 13 kW generator connected to a 220V/50Hz grid. The machine's parameters are presented below :

R_s=0.05Ω ; R_r=0.38Ω ; M=47.3mH ; L_s=50mH ; L_r=50 mH ; J=0.5kg.m² ; f=0.0035N.m.s^{-1}

The regulators will be tested and compared in three different configurations : reference tracking, sensitivity to perturbations and robustness against parameters variations.

4.1 Reference tracking

The machine is first placed in ideal conditions and is driven to 3500 rpm. We impose an active power step of -5kw at t=3s and we observe the response obtained respectively with the PI and the RST controller. Results are presented on figures 9 and 10.

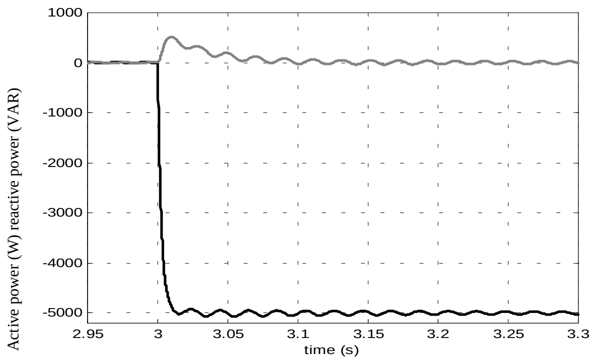

Fig. 9 : Response to an active power impact (PI controller)

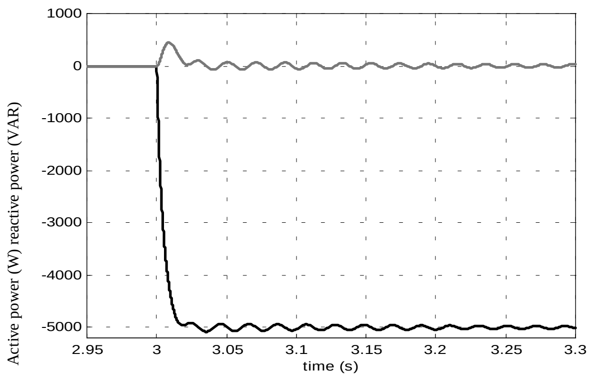

Fig. 10 : Response to an active power impact (RST controller)

We can notice that the response times are equivalent (about 10 ms). The effect of the active power step on the reactive power shows that the cross-coupling terms are a little bit better rejected with an RST controller than with a PI controller. The same test has been realized with a step of reactive power and the obtained performances are equivalent.

4.2 Sensitivity to perturbations

The generator is now driven at 3500 rpm with a constant reference of active power of –5 kW and a reactive power reference set to zero. At t=3s, the speed suddenly varies from 3500 to 3100 rpm. This speed impact can be compared to a wind gust in a real wind energy system. The effect of this speed step on the behavior of the power generated is shown on figures 11 and 12 for the two controllers.

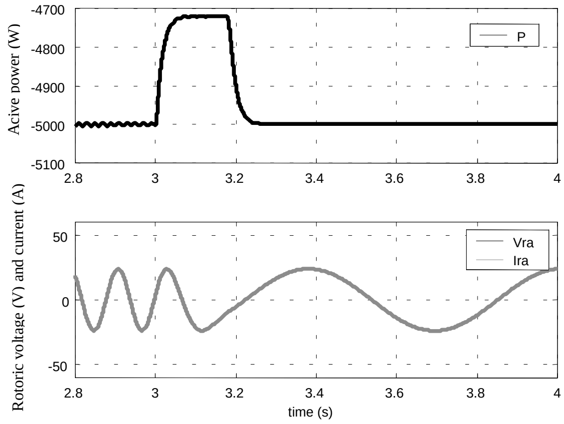

Fig. 11 : Response to a speed impact (PI controller)

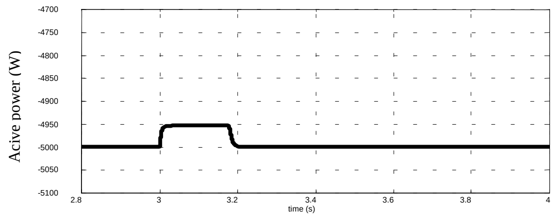

Fig. 12 : Response to a speed impact (RST controller)

These results permit to verify that the RST controller has better performances than PI to reject speed perturbation. As a matter of fact, the variation of active power is about 80 per cent smaller with the RST than with the PI controller. We also show the waveforms of rotoric voltage and current on figure 11. The variation of frequency is naturally related to the speed variation.

4.3 Robustness

In order to test the robustness of the two controllers, the value of the rotoric resistance R_r is doubled (from 0.38Ω to 0.76Ω). The generator is driven to 3500 rpm and we impose an active power reference of -5kW. Figures 13 and 14 show the effect of rotoric resistance variation on the generator response for the two controllers.

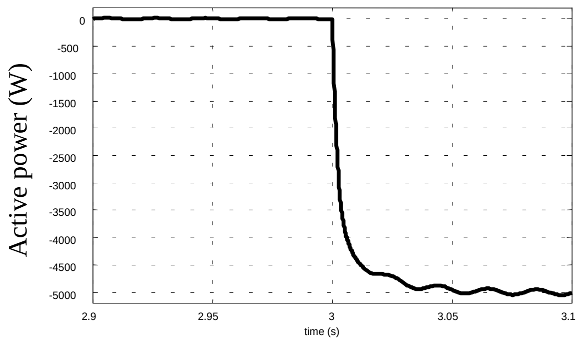

Fig. 13 : Response to a rotoric resistance variation (PI controller)

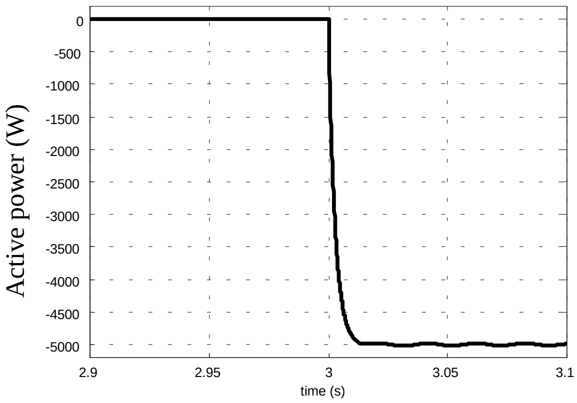

Fig. 14 : Response to a rotoric resistance variation (RST controller)

This robustness test shows that in the case of a PI regulator, the time response is strongly altered whereas it remains unmodified when the RST controller is used.

5. CONCLUSION

This paper has presented a device intended to fit in a wind mill based on a Doubly Fed Induction Generator connected to the grid. After a description of this device and its connection procedure, we have established a two-phase mathematical model of the DFIG. In order to control statoric active and reactive power exchanged between the DFIG and the grid, a vector-control strategy has been presented. Simulations have been investigated with two types of regulators: classical proportional-integral and polynomial RST based on pole-placement theory. The synthesis of the RST controller has been detailed. Simulations results have shown that performances are equivalent for the two controllers under ideal conditions (no perturbations and no parameters variations). The RST controller is more efficient when the speed is suddenly changed (which happens frequently in wind energy conversion systems) and is more robust under parameters variations of the DFIG (for example rotoric resistance in our study).

6. REFERENCES

[1] S. Heier, "Grid integration of wind energy conversion systems.", John Wiley & Sons Ltd, England, 1998.

[2] L. Xu, W. Cheng, "Torque and reactive power control of a doubly-fed induction machine by position sensorless scheme.", IEEE Transactions on Industry Applications, Vol. 31, N°3, pp 636-642, May/June 1995.

[3] M. Yamamoto, O. Motoyoshi, "Active and reactive power control for doubly-fed wound rotor induction generator.", IEEE Transactions on Power Electronics, Vol. 6, N°. 4, Oct. 1991, pp 624-629.

[4] M. B. Rifai, T. H. Ortmeyer, "Dynamic analysis of a doubly fed generator in power system applications.", Electric Machines and Power Systems, Vol. 21, pp 141-150, 1993.

[5] B. Hopfensperger, D.J. Atkinson, R.A. Lakin, : "Stator-flux-oriented control of a doubly fed induction machine with and without position encoder.", IEE Proc.-Electr. Power Appl., Vol. 147, N°. 4, July 2000, pp 241-250.

[6] L. Morel, A. Mirzaian, J.M. Kauffmann: "Field oriented control for double fed induction machine : simulation and experimental results.", ELECTRIMACS'96., Vol. 2, September 17-18-19, 1996, pp 391,396.

[7] D. Ramuz, A. Mirzaian, J.M. Kauffmann, S. Tnani, H. Godfroid : "Control strategy of double fed machine for variable speed drives.", proceedings of ICEM 98, Istanbul, Sept. 1998, pp. 1340-1345.

[8] P. De Larminat, "Automatique – Commande des systèmes linéaires", Seconde Edition 1997 Hermes.

ACKNOWLEDGMENTS

The authors gratefully acknowledge financial support from the French Agency for Environment and Energy Management "ADEME", the french company "Leroy-Somer" and the french regional council of "Pays de la Loire".